

$$y = a(1 - \exp(-bx))$$

where a and b are regression coefficients.

The conduction velocity (CV) was calculated as the distance traveled normal to isochrones of activation per unit time. The CVs in the unstretched state and stretched state are defined as follows ⁵:

$$CV_{unstretched} = \frac{L_0}{\Delta t(L_0)}$$

$$CV_{stretched} = \frac{L_0}{\Delta t(L_1)}$$

where $\Delta t(X)$ is the conduction time measured over the two-point distance X. L_0 and L_1 are the unstretched and stretched two-point distances, respectively.

The relationships between the thickness and the strain and between the normalized dF/dt max and the local strain were assessed by univariate linear regression analysis and the Pearson correlation coefficient test. A repeated-measures ANOVA was used to evaluate the drug effects. When there was a significant difference, Tukey's test was applied for multiple comparisons. In the whole heart preparations, difference in the excitation probability among four groups of normalized thickness was analyzed by one-way ANOVA followed by Bonferroni's test. Data were expressed as means \pm SEM. Values of $P < 0.05$ were considered statistically significant.

Supplemental References

1. Inagaki M, Hidaka I, Aiba T, Tatewaki T, Sunagawa K, Sugimachi M. High resolution optical mapping of cardiac action potentials in freely beating rabbit hearts. *Conf Proc IEEE Eng Med Biol Soc.* 2004;5:3578-3580.
2. Gray RA, Pertsov AM, Jalife J. Spatial and temporal organization during cardiac fibrillation. *Nature.* 1998;392:75-78.
3. Caldwell RA, Clemo HF, Baumgarten CM. Using gadolinium to identify stretch-activated channels: technical considerations. *Am J Physiol.* 1998;275:C619-621.
4. Kiseleva I, Kamkin A, Wagner KD, Theres H, Ladhoff A, Scholz H, Gunther J, Lab MJ. Mechanoelectric feedback after left ventricular infarction in rats. *Cardiovasc Res.* 2000;45:370-378.
5. Mills RW, Narayan SM, McCulloch AD. The Effects of Wall Stretch on Ventricular Conduction and Refractoriness in the Whole Heart. In: Kohl P, Sachs F, Franz MR, eds. *Cardiac Mechano-Electric Feedback and Arrhythmias: From Pipette to Patient.* Philadelphia: Elsevier Saunders; 2005:127-136.

Supplemental Figure Legends

Online Figure I. Tissue preparation and the experimental setup.

A: A photograph of the tissue preparation. Scale bar: 5 mm.

B: Schematic representation of the experimental setup. The excised RV wall with its intact coronary artery is glued to a pair of tissue supports connected to a force transducer (FT) and a linear motor (LM). ECG, force (*f*) and displacement (*d*) signals are amplified (Amp) and recorded by an AD converter (A/D) and personal computer (PC). Stretch and electrical stimulation commands are generated by the PC and applied to the LM and an electrical stimulator (Stim) through a DA converter (D/A). For optical mapping, the tissue is illuminated by light emission diodes (LED). The fluorescent emission light is split by a dichroic mirror (DM) and narrowed down to two frequency bands by appropriate filters (F1 and F2). Optical images are captured by two independent CMOS cameras (CMOS) with image intensifiers (I.I) and stored in a memory controller (M/C) and the PC. L: lens.

Online Figure II. Action potential shapes of tissues and whole heart preparations.

Upper figure: Representative optical signals initiated by an electrical stimulus are shown for a tissue (left) and a whole heart preparation (right). Lower figure: 50% repolarizations of the action potential duration (APD₅₀) are shown for a tissue and a whole heart preparation. Scale bar: 100 ms. NS: no significance.

Online Figure III. Experimental setup for the whole heart study.

A: Schematic representation of the experimental setup. A balloon (B) is inserted into the RV of the perfused whole heart. The balloon is connected to a piston pump (P) with a linear motor (LM). ECG and volume (*V*) signals are amplified (Amp) and recorded by an AD converter (A/D) and a personal computer (PC). Stretch and electrical stimulation commands are generated by the PC and applied to the LM and an electrical stimulator (Stim) through a DA converter (D/A). For optical mapping, the heart is illuminated by light emission diodes (LED). The fluorescent emission light is split by a dichroic mirror (DM) and narrowed down to two frequency bands by appropriate filters (F1 and F2). Optical images are captured by two independent CMOS cameras (CMOS) with image intensifiers (I.I) and stored in a memory controller (M/C) and the PC. L: lens.

Online Figure IV. Stretch and volume pulse protocols.

In both tissue and whole heart studies, a stretch/volume pulse (S₂) is preceded by a train of pulses (S₁: 2 Hz) to stabilize the heart conditions. In the tissue study (A), the coupling interval between the last S₁ and S₂ (I₂) is set at 500 ms. The plateau (P) and velocity (V) of the stretch are 50 ms and 0.5%/ms, respectively. The amplitude of the stretch (E) is set at 5%, 10%, 15%, 20%, 25% or 30% of the tissue length. In the whole heart study (B), two different protocols were applied (a and b). In protocol (a), the coupling interval between the last S₁ and S₂ (I₂) was set at 500 ms and the entire

duration (T) and the speed (V) of the volume pulses were set at 60 ms and 0.1 ml/ms, respectively. The amplitude of the volume pulses (E) was set at 0.5, 1.0, 1.5 or 2.0 ml. In protocol (b), I2 was varied from 90 to 130 ms. The entire duration (T) and the speed (V) of the volume pulses were set at 50 ms and 0.2 ml/ms, respectively. The amplitude of the volume pulses (E) was set at 1.0, 1.5 or 2.0 ml.

Online Figure V. Excitation and its modulation by shorter stretches.

A: Representative isochronal maps of optical mapping data in response to 10% and 25% stretches with a shorter entire time duration (50 ms). Scale bar: 4 mm. **B:** Ratiometric optical signals in response to 10% and 15% stretches with various timings (phases 2, 3 and 4) during the cardiac cycle. The transient stretch applied in phase 2 elicited a repolarization. The transient stretch applied in late phase 3 or phase 4 elicited a depolarization which was sometimes followed by a premature ventricular contraction. Scale bar: 50 ms.

Online Figure VI. Stretch-induced excitation from the center and conduction velocity.

A: Left panel: Representative isochronal maps of a membrane potential showing the focal excitation from the center region initiated by a 15% stretch. Right panel: Corresponding thickness distributions. Scale bar: 2 mm. **B:** a, Comparison of the vertical CVs between the excitations initiated by an electrical stimulus (electric stim) and a 10% stretch. b, Comparison of the horizontal CVs between the excitations initiated by an electrical stimulus and a 10% stretch. Left panels: Representative isochronal maps for the electrical stimuli. Right panels: Representative isochronal maps for the 10% stretches. Scale bar: 4 mm.

Online Figure VII. Relationship between dF/dt maximums and local strains.

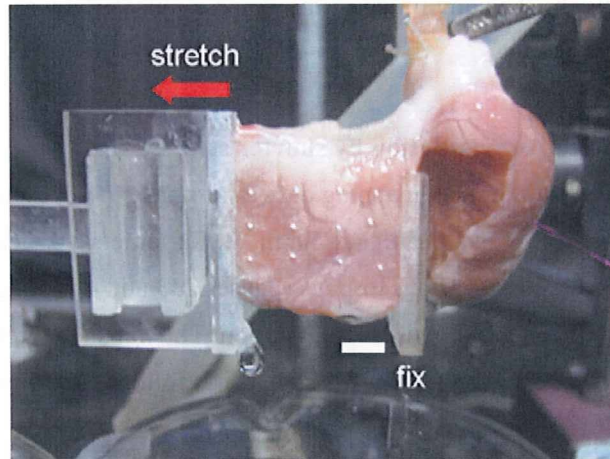
Relationships between the normalized dF/dt max (maximum value of the time derivative of the ratiometric optical signal) of the action potential upstrokes and local strains in response to 10% (open circle), 20% (closed black rectangle) and 30% (closed gray square) stretches. Line is a linear regression line (n=5, r=-0.40, P<0.0001).

Online Figure VIII. Phase dependency of the stretch-induced excitations

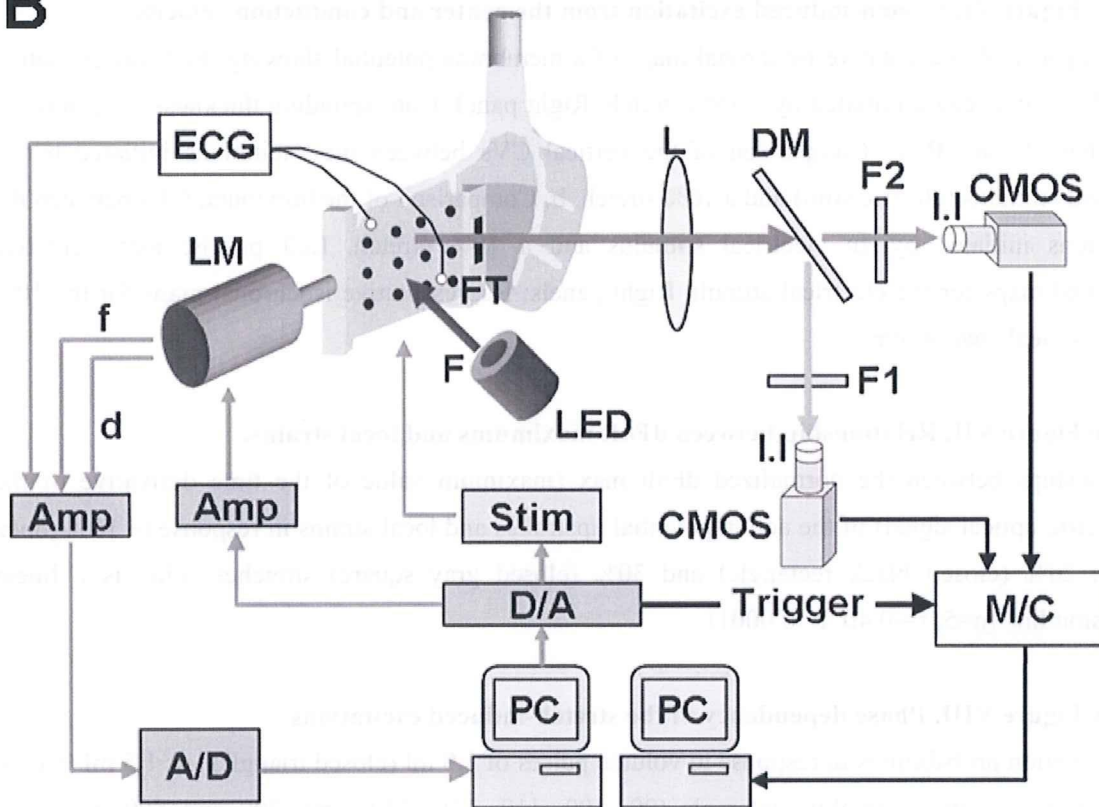
The excitation probabilities in response to volume pulses of 1.0 ml (closed triangles) or 1.5 ml (closed squares) with various coupling intervals (90, 100, 110, 120, 130, 150, 200 and 500 ms) were evaluated.

Supplemental Figures

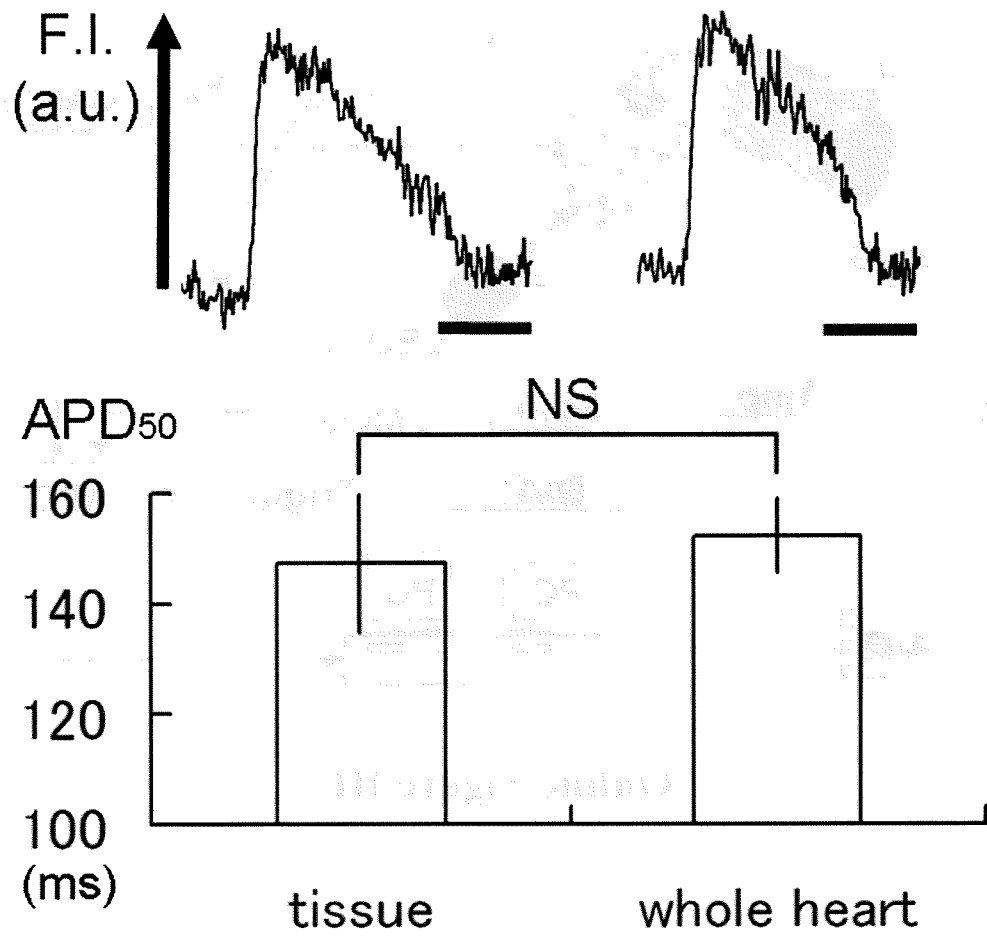
A



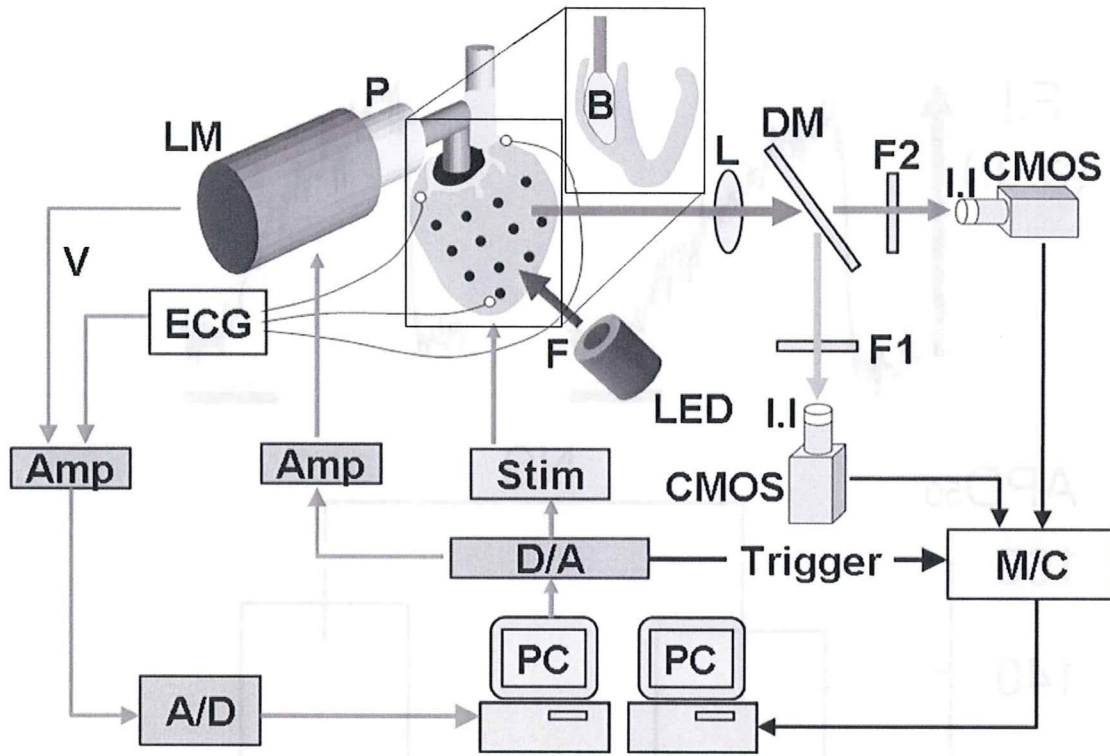
B



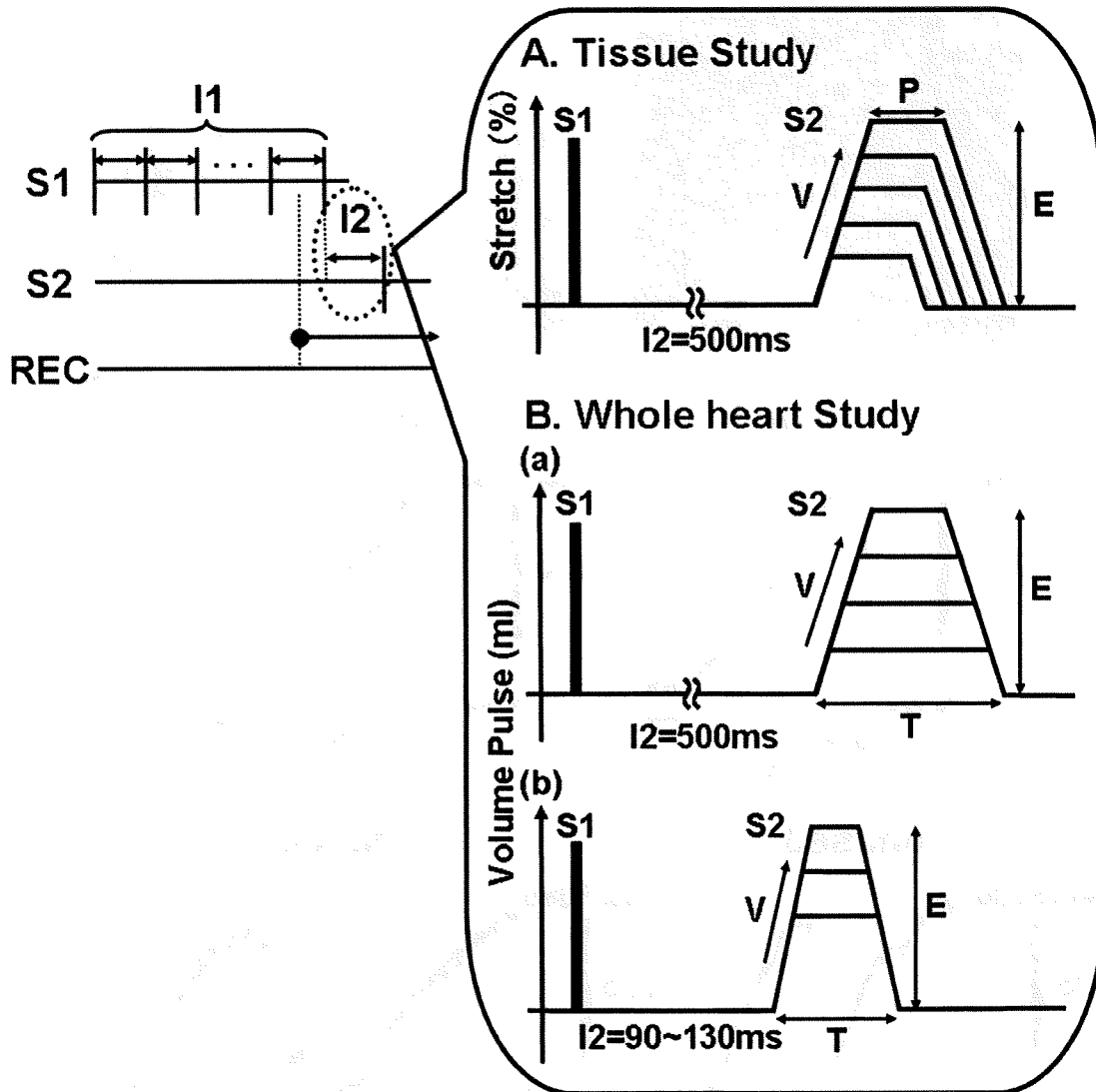
Online Figure I



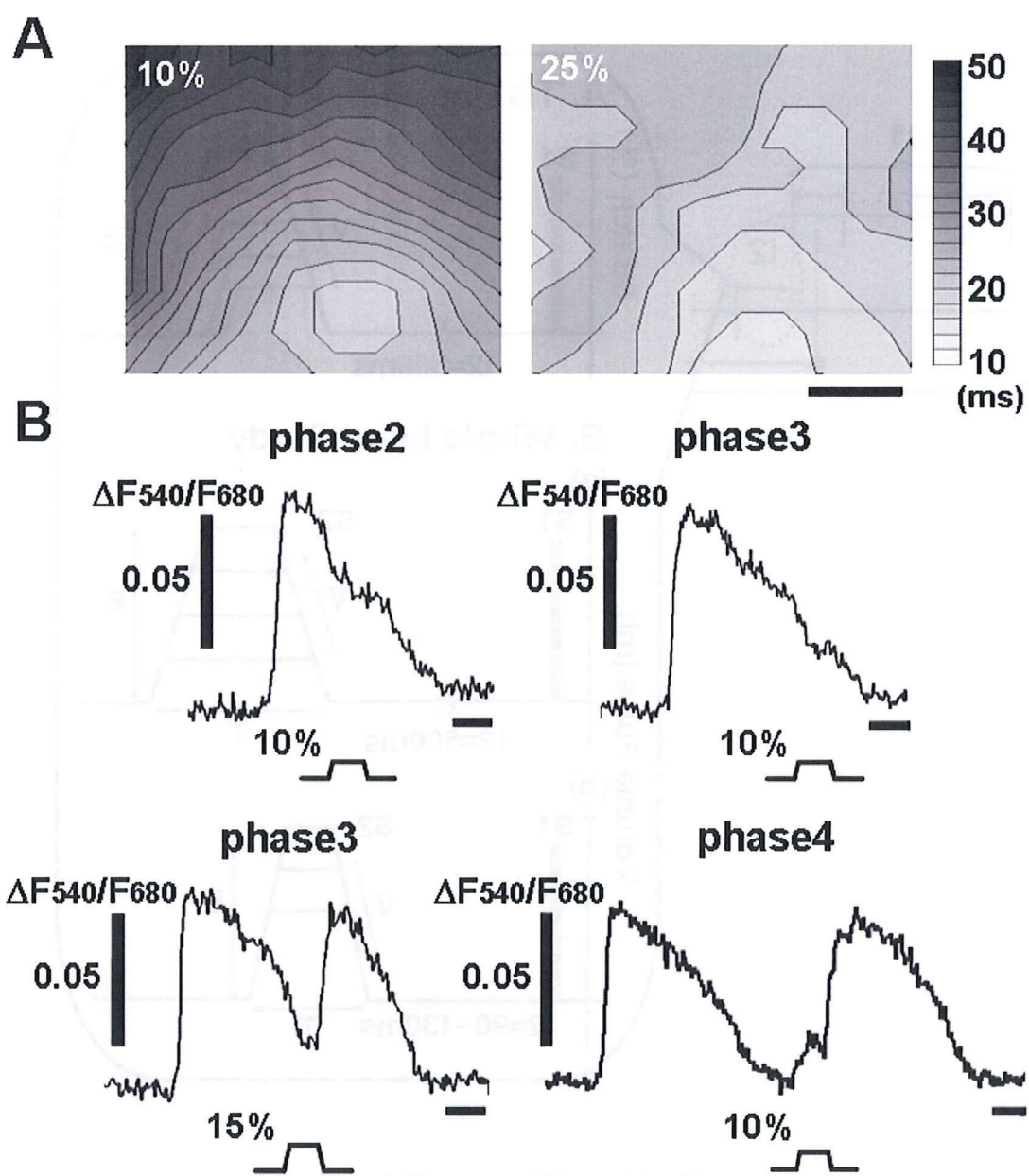
Online Figure II



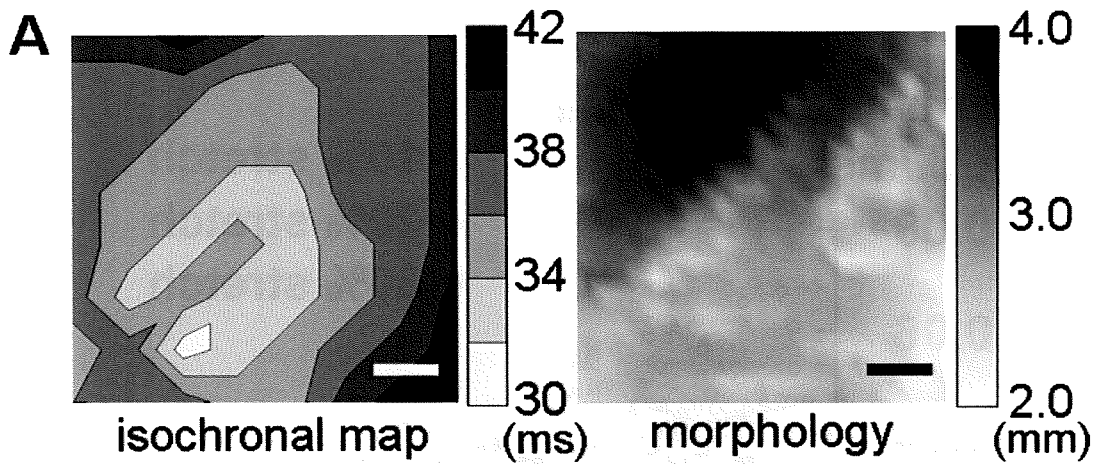
Online Figure III



Online Figure IV



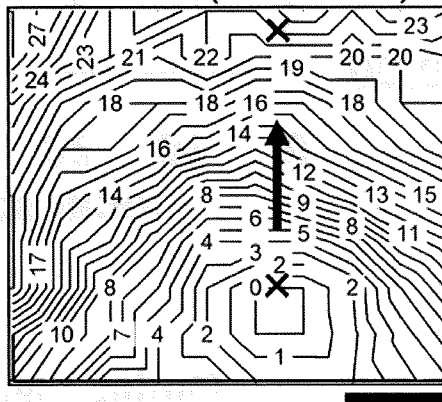
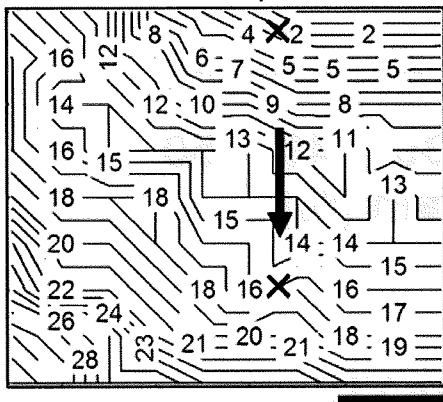
Online Figure V



B (a) vertical direction

electric stim ($v=0.63\text{m/s}$)

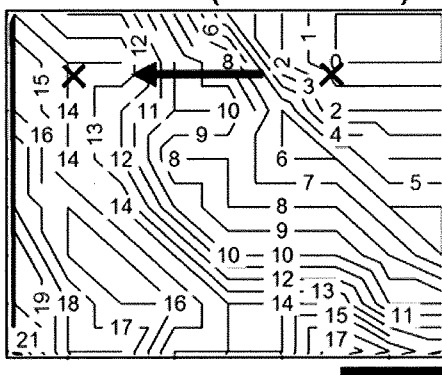
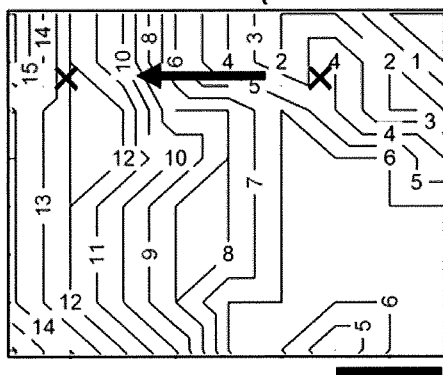
stretch ($v=0.43\text{m/s}$)



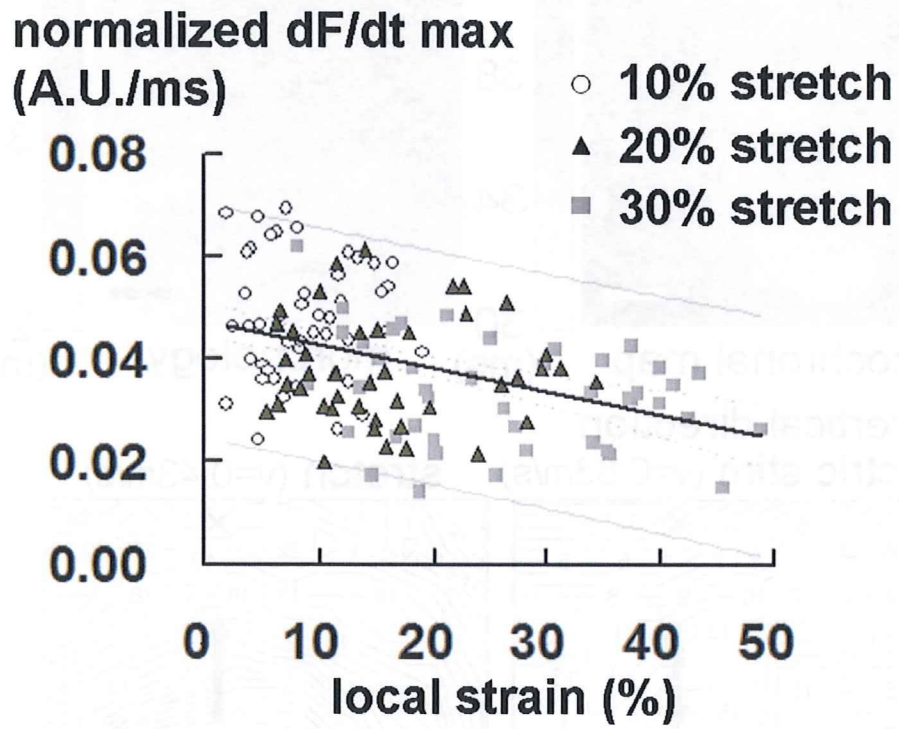
(b) horizontal direction

electric stim ($v=1.19\text{m/s}$)

stretch ($v=0.73\text{m/s}$)

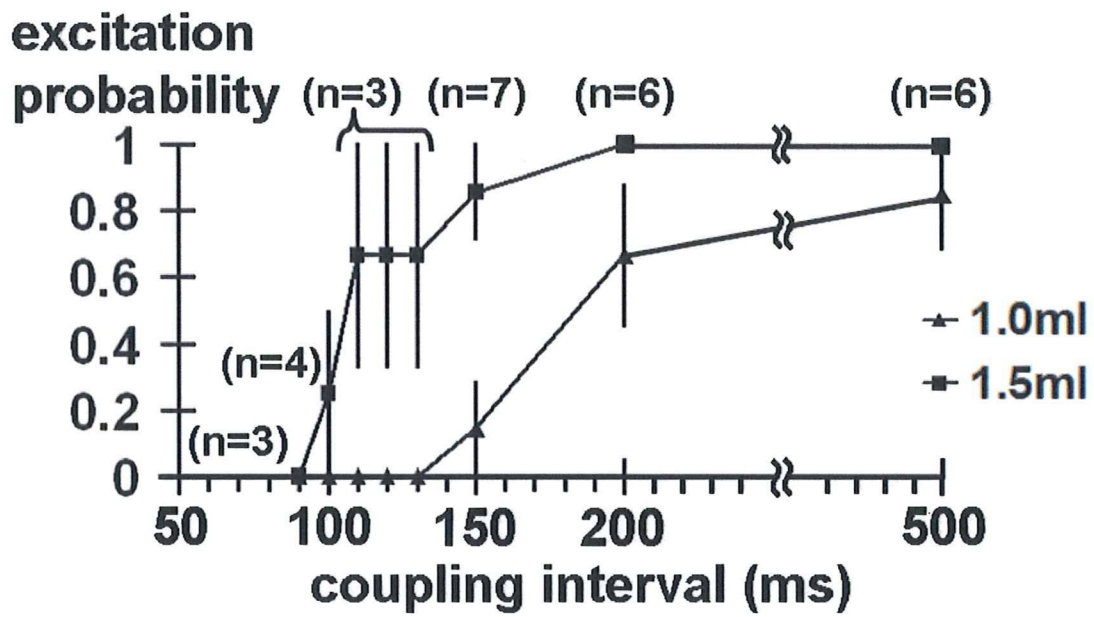


Online Figure VI



Online Figure VII





Online Figure VIII

Bionic Cardiology: Exploration Into a Wealth of Controllable Body Parts in the Cardiovascular System

Masaru Sugimachi, *Member, IEEE*, and Kenji Sunagawa, *Senior Member, IEEE*

Clinical Application Review

Abstract—Bionic cardiology is the medical science of exploring electronic control of the body, usually via the neural system. Mimicking or modifying biological regulation is a strategy used to combat diseases. Control of ventricular rate during atrial fibrillation by selective vagal stimulation, suppression of ischemia-related ventricular fibrillation by vagal stimulation, and reproduction of neurally commanded heart rate are some examples of bionic treatment for arrhythmia. Implantable radio-frequency-coupled on-demand carotid sinus stimulators succeeded in interrupting or preventing anginal attacks but were replaced later by coronary revascularization. Similar but fixed-intensity carotid sinus stimulators were used for hypertension but were also replaced by drugs. Recently, however, a self-powered implantable device has been reappraised for the treatment of drug-resistant hypertension. Closed-loop spinal cord stimulation has successfully treated severe orthostatic hypotension in a limited number of patients. Vagal nerve stimulation is effective in treating heart failure in animals, and a small-size clinical trial has just started. Simultaneous corrections of multiple hemodynamic abnormalities in an acute decompensated state are accomplished simply by quantifying fundamental cardiovascular parameters and controlling these parameters. Bionic cardiology will continue to promote the development of more sophisticated device-based therapies for otherwise untreatable diseases and will inspire more intricate applications in the twenty-first century.

Index Terms—Biological regulation, feedback control, implantable device, nerve stimulation, system identification.

I. INTRODUCTION

BIONIC cardiology can be defined as medical science in the field of cardiovascular medicine, which explores the electronic control of the body [1], [2]. The term “bionic” derives literally from “bio” (meaning life) and “-onic” (short for electronic). Utilizing the biological amplification mechanism of excitable membranes is an ingenious way to save power and ensure long-term operation of electronic devices. Therefore, the electronic controllers are usually designed to act on

specialized tissues such as nerves, skeletal muscles, and myocardium. Since the neural system acts as the control center of the biological regulatory systems, the most efficient way of intervening and controlling the body is to manipulate the neural system.

In the earlier studies of our groups, we defined bionic cardiology in a narrower sense. In developing methods to artificially reconstruct functional defects such as severe orthostatic hypotension (due to loss of pressure stabilization function), we attempted to mimic the biological regulation as precisely as possible [3]–[6] (Fig. 1). To accomplish this, we applied the white-noise approach to unveil the detailed characteristics of complexly integrated biological regulation [4], [7]–[14]. Therefore, by “bionic” cardiology, we meant the reproduction of biological regulation. Although it is not always true (see below), through our efforts in reproducing biological regulation, we began to take full advantage of control engineering in developing artificial controllers. This breakthrough made it possible for us to design feedback closed-loop control rather than open-loop control to achieve therapeutic goals.

Later, we learned that only mimicking biological regulation is not sufficient in treating common diseases. Our body is often affected by common diseases despite the presence of normally functioning biological regulation. In other words, under certain pathophysiological conditions, the normal biological regulation fails to accommodate disease conditions. In some diseases such as heart failure, the biological regulation system may in fact participate in the process of disease evolution and progression. This is best illustrated by the fact that heart failure can be treated with drugs that antagonize biological regulation. Therefore, the strategy to combat these “common” diseases should go beyond the restoration of normal biological regulation. We do not have any model at hand to learn from. In treating common diseases, one has to modify the biological regulation rather than to mimic physiological regulation.

In this paper, we attempt to discuss bionic cardiology in a broader sense, for the reason mentioned above. We also include some earlier studies of open-loop or on-demand control; these examples may serve as a basis for the development of more sophisticated feedback controllers by contemporary control engineering. How we choose short-term therapeutic targets for the feedback control remains a vital question, as the short-term targets are only a proxy for the true endpoint; namely, survival. Nevertheless, the clinical outcome of the predefined target can be appropriately examined only with feedback control.

Manuscript received August 15, 2009. First published October 16, 2009; current version published December 01, 2009. This work was supported in part by the Japan Society for the Promotion of Science under Grant-in-Aid for Scientific Research (S) 18100006 and by the Ministry of Health Labour and Welfare of Japan under Health and Labour Sciences Research Grants H19-nano-ippan-009 and H20-katsudo-shitei-007.

M. Sugimachi is with the Department of Cardiovascular Dynamics, Advanced Medical Engineering Center, National Cardiovascular Center Research Institute, 5658565 Suita, Japan (e-mail: su91mach@ri.ncvc.go.jp).

K. Sunagawa is with the Department of Cardiovascular Medicine, Graduate School of Medical Sciences, Kyushu University, 8128582 Fukuoka, Japan (e-mail: sunagawa@cardiol.med.kyushu-u.ac.jp).

Digital Object Identifier 10.1109/RBME.2009.2034623

1937-3333/\$26.00 © 2009 IEEE

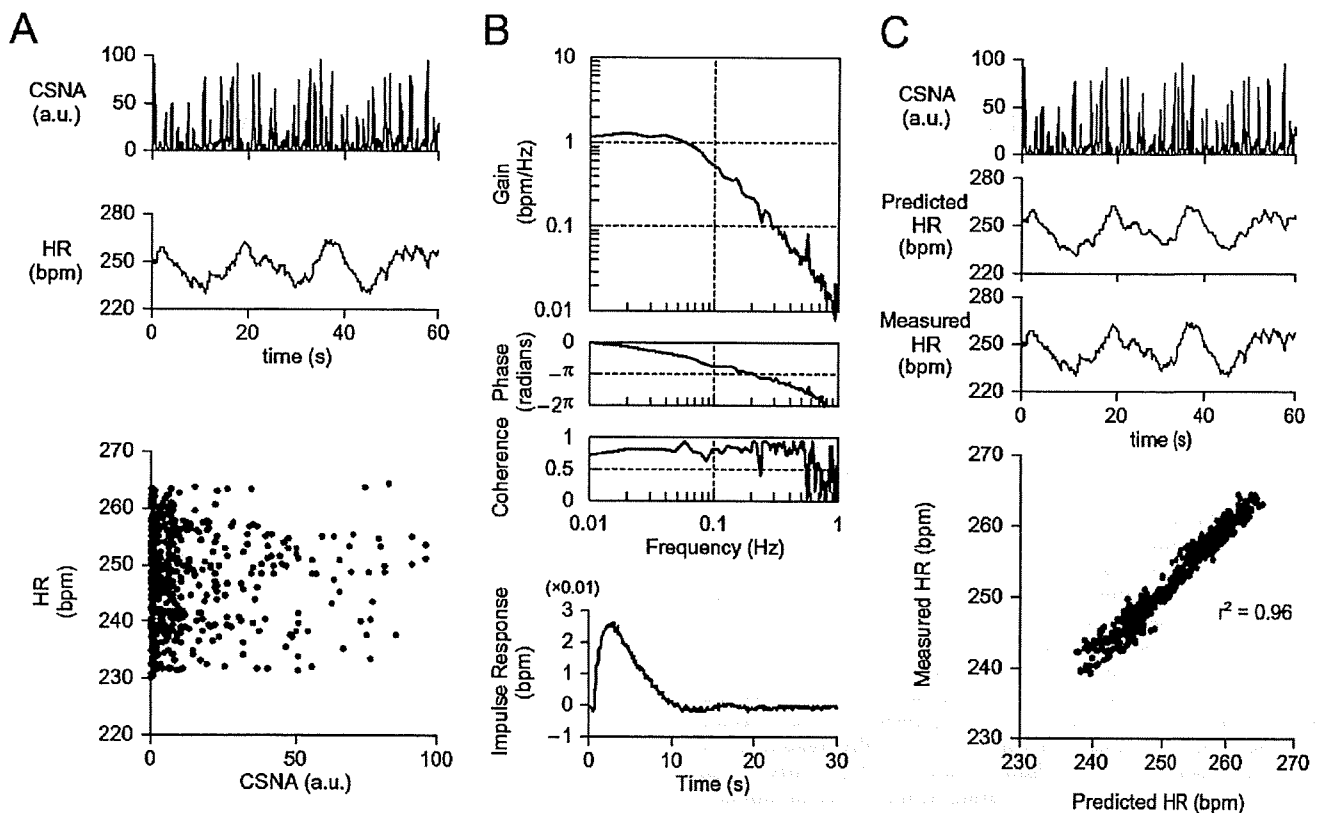


Fig. 1. A representative example of bionic cardiac pacemaker, i.e., neurally regulated pacemaker in a rabbit. (A) Simultaneously measured cardiac sympathetic nerve activity (CSNA) and heart rate (HR). Simple scattergram identified no obvious relationship. (B) Identified linear transfer function and corresponding impulse response to be used for decoding CSNA. (C) Decoded HR (predicted HR) from CSNA correlated well with measured HR. (Reproduced from [1] with permission.)

II. TREATMENT OF ANGINA PECTORIS

Angina pectoris is one form of ischemic cardiac diseases. This may manifest as a chronic stable form for years. Destabilization of atherosclerotic plaques may precipitate acute myocardial infarction resulting in irreversible myocardial loss. In unstable angina, there is an imbalance between oxygen supply and demand and an absolute shortage of coronary blood flow. In the stable form, however, the anginal attack occurs as a result of demand ischemia, usually associated with exertion, emotional stress, and exposure to cold environment. Therefore, a reduction in oxygen demand benefits patients with stable angina. In fact, antianginal drugs such as nitrates and beta-adrenergic blockers are believed to relieve angina by reducing oxygen demand.

A. Carotid Sinus Nerve Stimulation

The treatment of angina by neural intervention was first performed by manual massage of the carotid sinus [15], where the mechanoreceptor exists to feedback-control the autonomic tone. In 1967, Braunwald *et al.* [16] electrically stimulated carotid sinus nerves in two patients with angina, in the same year as Schwartz *et al.* [17] did in patients with hypertension. They used radio-frequency (RF)-coupled neurostimulators. Briefly, the implanted part of the device consisted of two pairs of bipolar platinum electrodes (for bilateral stimulation), coiled stainless steel leads, and a receiver unit. An external battery-driven transmitter delivered RF impulses transcutaneously through an antenna placed just above the receiver.

Carotid sinus nerve stimulation reflexly inhibits sympathetic activity and decreases myocardial oxygen consumption by lowering blood pressure, heart rate, and contractility. Enhanced vagal activity decreases heart rate and may directly decrease contractility [18] in the presence of a high sympathetic tone. Braunwald's group reported that on-demand use of carotid sinus nerve stimulation almost instantly aborted existing anginal attack and prevented the occurrence of new ones [16], [19]. Mason *et al.* [20] compared the effects of nitrates, beta-blockers, and carotid sinus nerve stimulation. Carotid sinus nerve stimulation was considered to reduce preload (as nitrates) and have negative chronotropic and inotropic (as beta-blockers) effects. Vatner *et al.* [19], [21] demonstrated in chronically instrumented conscious dogs that carotid sinus nerve stimulation lowered the resistance of various vascular beds. Of note, coronary vascular resistance also decreased while oxygen demand decreased and was considered to be mediated by sympathetic withdrawal. Solti *et al.* [22], [23] observed that carotid sinus nerve stimulation preferentially increased blood flow in ischemic areas. They attributed this observation to vasodilatation of collateral vessels.

In 1969, Epstein *et al.* [24], [25] treated 17 patients with drug-resistant angina using carotid sinus nerve stimulation. They observed symptomatic relief in 13 of their patients. Angina-interruptive and -prophylactic use of carotid sinus nerve stimulation prolonged exercise duration in 10 and 12, respectively, of the 13 patients. Carotid sinus stimulation had transient adverse effects (pain, cough, paresthesia, and neck tightness sensation; only for around four weeks) that were milder than those

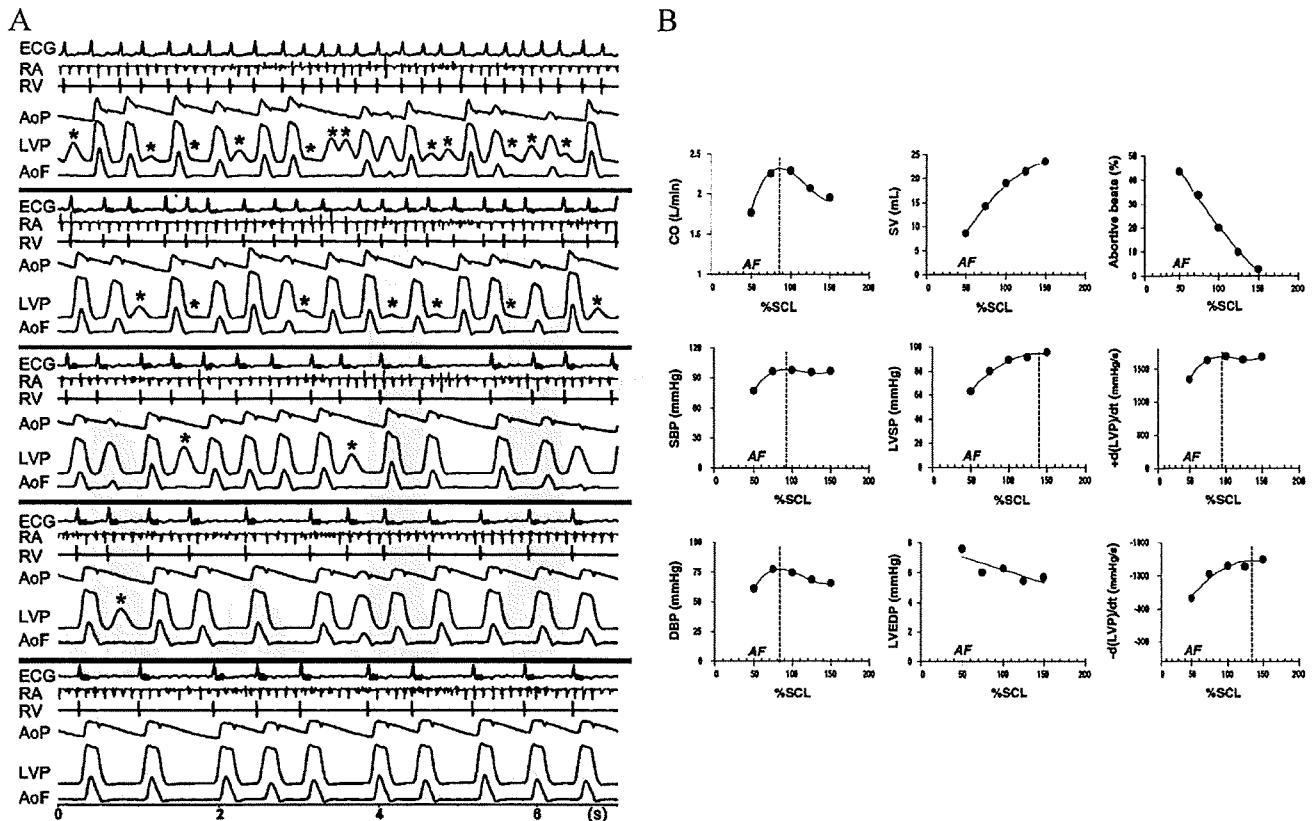


Fig. 2. (A) A representative example of controlling ventricular rate in a dog with atrial fibrillation (AF) by electrical stimulation of vagal nerve at epicardial fat pad innervating atrioventricular node. From top: no control, control to 75%, 100%, 125%, 150% of sinus cycle length (SCL). RA: intracardiac ECG from RA; RV: intracardiac ECG from RV; AoP: aortic pressure; LVP: left ventricular pressure; AoF: aortic flow; (*) abortive beats. (B) Effects of ventricular rate control by fat pad stimulation on hemodynamics in ten dogs. CO: cardiac output; SBP: systolic blood pressure; DBP: diastolic blood pressure; SV: stroke volume; LVSP: left ventricular systolic pressure; LVEDP: left ventricular end-diastolic pressure; $+d(LVP)/dt$, maximal rate of rise in left ventricular pressure; $-d(LVP)/dt$, minimal rate of fall in left ventricular pressure. (Reproduced from [33] with permission.)

of vagal stimulation (vomiting, salivation, coughing) [19], [26]. Detailed surgical techniques for carotid sinus stimulation have been described [19], [26]. Carotid sinus nerve stimulation was performed in various institutes worldwide [27]–[29].

Further development of neurostimulator treatment of angina by directly manipulating the autonomic tone is not currently underway, as coronary revascularizations (percutaneous coronary intervention and bypass graft) and potent drugs have become the standard treatments of choice. Recently, however, spinal-cord stimulation used to relieve anginal pain in advanced ischemic heart disease has been reported to also improve some indexes of heart performance [30].

III. TREATMENT OF ARRHYTHMIAS

Various forms of arrhythmia have been treated by stimulation of carotid sinus nerves and vagal nerves. Stimulation of carotid sinus nerves involves both the reflex-mediated inhibition of sympathetic nerves and activation of vagal nerves. Heidorn *et al.* [31] showed that massage of the carotid sinus in normal subjects changed the electrocardiogram and concluded that the carotid sinus baroreflex is a physiological phenomenon.

A. Carotid Sinus Nerve Stimulation

Carotid sinus massage was frequently used for bedside diagnosis and treatment of supraventricular tachyarrhythmias

[32] in the era when diagnostic tools and antiarrhythmic drugs were limited. Later, Braunwald *et al.* [19] treated patients with supraventricular tachycardia by electrical carotid sinus nerve stimulation, using the same electronic device (Angistat, Medtronic) as used for the treatment of angina (see Section II for details). The authors concluded that electrical stimulation might reduce potential risks such as stroke associated with carotid sinus massage.

B. Vagal Nerve Stimulation

Direct electrical stimulation of the vagal nerve has once been abandoned due to frequent adverse effects. Vagal stimulation, however, has continued to attract the interest of cardiologists for the treatment of refractory arrhythmias including atrial fibrillation and/or life threatening arrhythmias (ventricular fibrillation). Mazgalev *et al.* [33]–[35] (Fig. 2) demonstrated in 18 dogs with simulated atrial fibrillation that electrical stimulation (Itrel II 7424, Medtronic; Photon ICD, St. Jude Medical) of the epicardial fat pad (at the junction of inferior vena cava and left atrium) was able to feedback-control the ventricular rate from 192 to 153 bpm at five weeks. The anatomical selectivity of vagal stimulation in targeting the atrioventricular conduction pathway suggested a minimum risk of adverse effects. In fact, the investigators continued this treatment for five weeks to six months in conscious dogs and reported no noticeable adverse

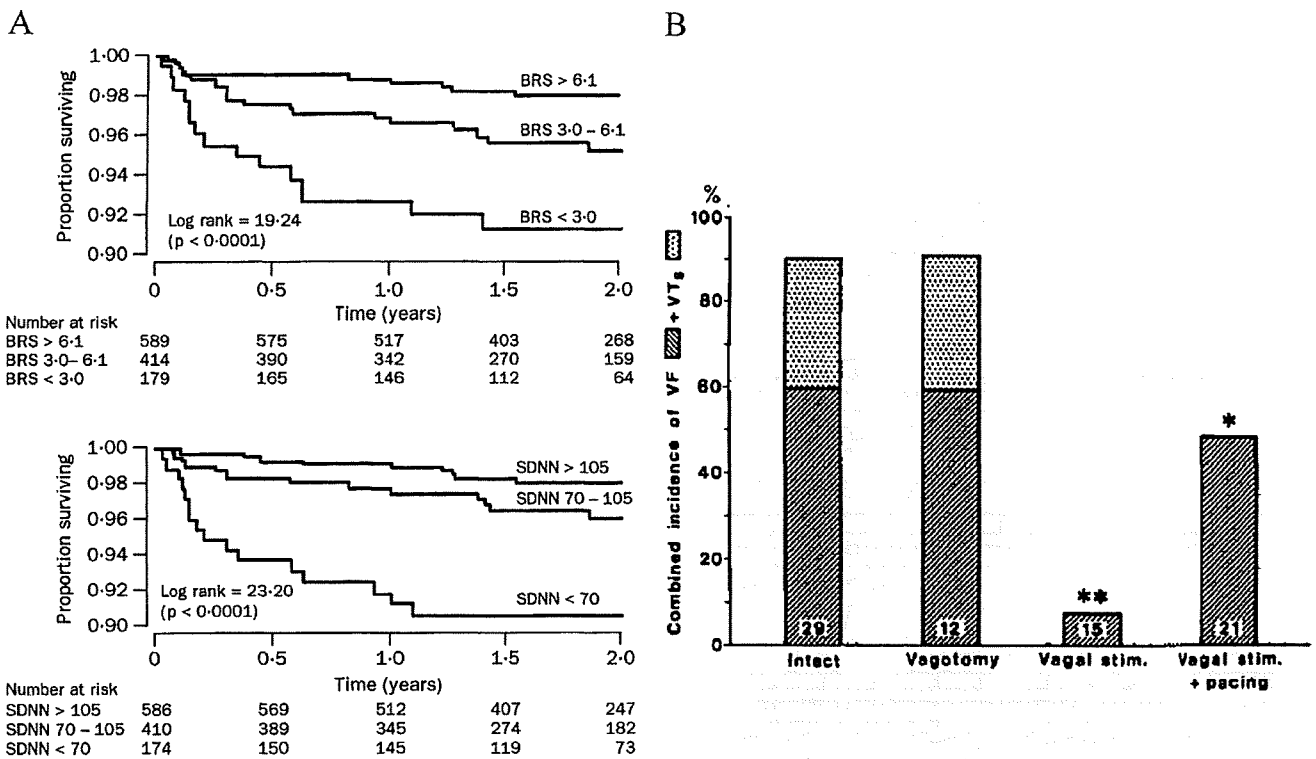


Fig. 3. (A) Survival (free from cardiac death or aborted cardiac arrest) in patients after myocardial infarction, plotted by baroreflex sensitivity (BRS) or by heart rate variability (SDNN). (B) Effect of efferent vagal stimulation (with vagotomy) started soon before reperfusion on incidence of VF and sustained ventricular tachycardia (VTs) in cats with coronary occlusion and reperfusion. (*) $p < 0.005$ versus intact and $p < 0.05$ versus vagotomy. (**) $p < 0.001$ versus intact and vagotomy. (Reproduced from [43] (A) and [44] (B) with permission.)

effects [34]. They also proposed that the preservation of normal ventricular conduction pathway outweighed the hemodynamic effect of the loss of atrial contraction, as shown by comparing the rate control by fat pad stimulation and atrioventricular nodal ablation with right ventricular pacing [35], [36]. This finding is consistent with the equivalent outcomes of rate and rhythm control in recent large clinical trials [37]. Even in a patient with severe heart failure, short-term endocardial stimulation of fat pad has succeeded in rate control and eventual restoration from a decompensated state [38].

Vagal stimulation enhanced with choline esterase inhibitor, beta-adrenergic blocker, and/or calcium blocker has once been used to induce temporary asystole for surgical procedures [39]. Atrial vagal denervation (ablation) was attempted to prevent atrial fibrillation associated with excessive vagal activity but with limited success [40].

Using a clinically relevant disease model (healed anterior myocardial infarction superimposed with acute ischemia during exercise), Cerati and Schwartz [41] found that the residual vagal activity during ischemia protects against fatal ventricular fibrillation. The same group succeeded in quantifying the background vagal activity with baroreflex sensitivity index (increase in RR interval for a given increase in blood pressure). Higher pre- (>20 versus < 14 ms/mmHg) and postinfarction (>15 versus < 9 ms/mmHg) baroreflex sensitivity predicted resistance to ventricular fibrillation in dogs (risk of ventricular fibrillation, 35% versus 85%, and 20% versus 91%, respectively, both $p < 0.001$) [42]. In large clinical trials (ATRAMI), higher baroreflex sensitivity predicted better outcomes [43] [Fig. 3(A)].

The same group showed that electrical vagal stimulation even beginning just before reperfusion (i.e., at the end of ischemia) was protective against ventricular fibrillation during reperfusion [44] [Fig. 3(B)]. Ando *et al.* [45] proposed that vagal stimulation exerts anti-arrhythmogenic effects by preserving the functional connexin in intercellular junctions thereby maintaining synchronicity between myocardial cells.

C. Neurally Regulated Artificial Pacemaker

Artificial pacemakers are the ultimate solution for bradyarrhythmias. Although the pacemakers guarantee the rate of cardiac contractions, they are unable to reproduce native physiological rate regulation. Ikeda *et al.* [4] developed a pacemaker that reproduced physiological regulation of heart rate. They succeeded to decode the heart rate response from sympathetic nerve activity as the central message and found the decoding rule by a white-noise approach [4], [8], [9]. The root mean square error of heart rate control relative to the native heart rate was 1.4 to 6.6 bpm or $1.2 \pm 0.7\%$ of mean heart rate [4] (Fig. 1). The success of deciphering the central autonomic neural messages opens up new applications of regulating artificial organs directly by measuring the autonomic nervous activity. It allows the artificial organs to operate as if they are an integral part of the native system.

IV. TREATMENT OF HYPERTENSION

Hypertension is universally the most prevalent risk factor that aggravates atherosclerotic diseases. Despite numerous studies

over many years, the true cause of elevated blood pressure remains unsolved in most patients. Since lowering blood pressure delays the atherosclerotic process, numerous antihypertensive drugs have been developed and used clinically. Electronic treatment of hypertension was first developed for patients with severe drug-resistant hypertension at the time when fewer drugs were available. In recent years, however, the development of advanced neurostimulators as well as the recognition of a large population with drug-resistant hypertension have promoted the reappraisal of this device treatment.

A. Classical Neurostimulation

Hypertension has been treated electronically, almost exclusively by electrical stimulation of the carotid sinus nerve, which reflexly induces withdrawal of sympathetic nerve activity. Griffith *et al.* [46] investigated the effect of unilateral carotid sinus nerve stimulation in normal and renal hypertensive dogs. Except in hypertensive dogs with contralateral carotid sinus nerve sectioned, the hypotensive effect of carotid sinus nerve stimulation gradually decreased in 50 min. This attenuation may be partly due to the counteracting effect of remaining intact baroreflex components.

The first implantable carotid sinus neurostimulator was developed in the University of Minnesota by two surgeons [47]. This device delivered fixed-intensity stimulation synchronous to R wave to bilateral carotid sinus nerves. When evaluated in dogs, blood pressure was dramatically decreased in hypertensive dogs compared to normal dogs (systolic effect of 40–50 mm Hg versus 20 mmHg). Motivated by the study of direct carotid sinus nerve stimulation in man [48], Schwartz *et al.* [17] applied three types of baropacers (primary-celled, rechargeable, RF-coupled) to unilateral carotid sinus nerve in patients. In eight of 11 patients followed for five months to 2.5 years, the depressive effects persisted (systolic effect: 30–100 mmHg; diastolic effect: 24–80 mmHg). Agishi *et al.* [49] used mercury column as an on-off switch to automatically control pressure in dogs. Brest *et al.* [50] (eight patients) and Solti *et al.* [51] (one patient) described their experience of using a commercially available RF-coupled device (Barostat, Medtronic) for stimulating bilateral carotid sinus nerve. Using an externally worn transmitter, RF-coupled device allowed long-term treatment and external control of pulse amplitude and width. Electrical stimulation-induced hypotension was accompanied by bradycardia, a lower rate of pressure rise, lower cardiac index, and a decrease in vascular resistance relative to the level expected from significant hypotension.

Despite these earlier reports, device treatment of hypertension has almost disappeared until recently, due to the development of various classes of useful antihypertensive drugs. Moreover, in spite of reports of sustained hypotensive effect of carotid sinus nerve stimulation for over two years [50], arguments against the role of arterial baroreflex in chronic blood pressure regulation have gained widespread support. These arguments were based on the observation that blood pressure almost normalizes a few days after experimental sinoaortic denervation. This finding seemingly supports the notion of complete resetting of baroreflex and the role of the

renin-angiotensin-aldosterone system in maintaining long-term blood pressure.

B. Role of Baroreflex Revisited in the Pathogenesis of Hypertension

Recently, using a carotid sinus nerve stimulation with neurostimulator (CVRx), Lohmeier *et al.* [52]–[57] showed that seven days of carotid sinus nerve stimulation induced sustained decrease in blood pressure associated with decrease in plasma norepinephrine but without increase in renin activity, suggesting a powerful role of baroreflex in chronic arterial pressure regulation [Fig. 4(A)]. The authors suggested that decreased renal sympathetic activity inhibits the increase in renin secretion during hypotension and enhances renal sodium secretion. The hypotensive effect did not persist in angiotensin-induced hypertension due to increased angiotensin level and when sympathetic tone and renin level were already suppressed before carotid sinus nerve stimulation [53] but did persist in obesity-induced hypertension [56]. Carotid sinus nerve stimulation decreased blood pressure to a greater extent than complete beta- and alpha1-adrenergic blockade, suggesting the pathophysiological relevance of postsynaptic alpha2-adrenergic mechanism [57]. Based on these results, the authors concluded that baroreflex is involved in chronic pressure regulation. Even though the resetting of baroreceptors cannot be denied, central resetting of baroreflex seems very small.

Another line of evidence also supports the role of baroreflex in chronic pressure regulation. Thrasher [58]–[64] has shown that chronic baroreceptor unloading (baroreceptor denervation except one carotid sinus, and ligation of common carotid artery of the remaining innervated carotid sinus) produces rather different pressor response than sinoaortic denervation. Chronic baroreceptor unloading maintained pressor response for at least seven days [58] [Fig. 4(B)], and although pressor response was reduced at five weeks, the magnitude was significantly greater than that of sinoaortic denervation [62] (decreased response may be due to increased sinus pressure by back pressure). He attributed the difference between chronic baroreceptor unloading and sinoaortic denervation to central adaptation in sinoaortic denervation. Reports by Munch *et al.* [65] on incomplete (56%) chronic resetting also supported a role of baroreflex in chronic pressure regulation. Taken together, there is no question that baroreflex plays a significant role in chronic blood pressure regulation. Hence a new model of carotid sinus neurostimulator (Rheos, CVRx), which is an external RF signal controllable, self-powered implantable device with long-life battery, would be a powerful clinical tool in controlling drug-resistant hypertension.

Unlike fixed-intensity carotid sinus nerve stimulation, development of sophisticated real-time feedback closed-loop neurostimulator requires control engineering. In an old article by Warner [66], the author failed to attenuate externally imposed cyclic pressure disturbances by a simple increase in baroreceptor gain. He correctly attributed this to the delay in pressure regulation. On the contrary, Kubota *et al.* [3] have shown that properly identified baroreceptor transduction in terms of transfer function reproduces similar level of pressure stability as native baroreflex.

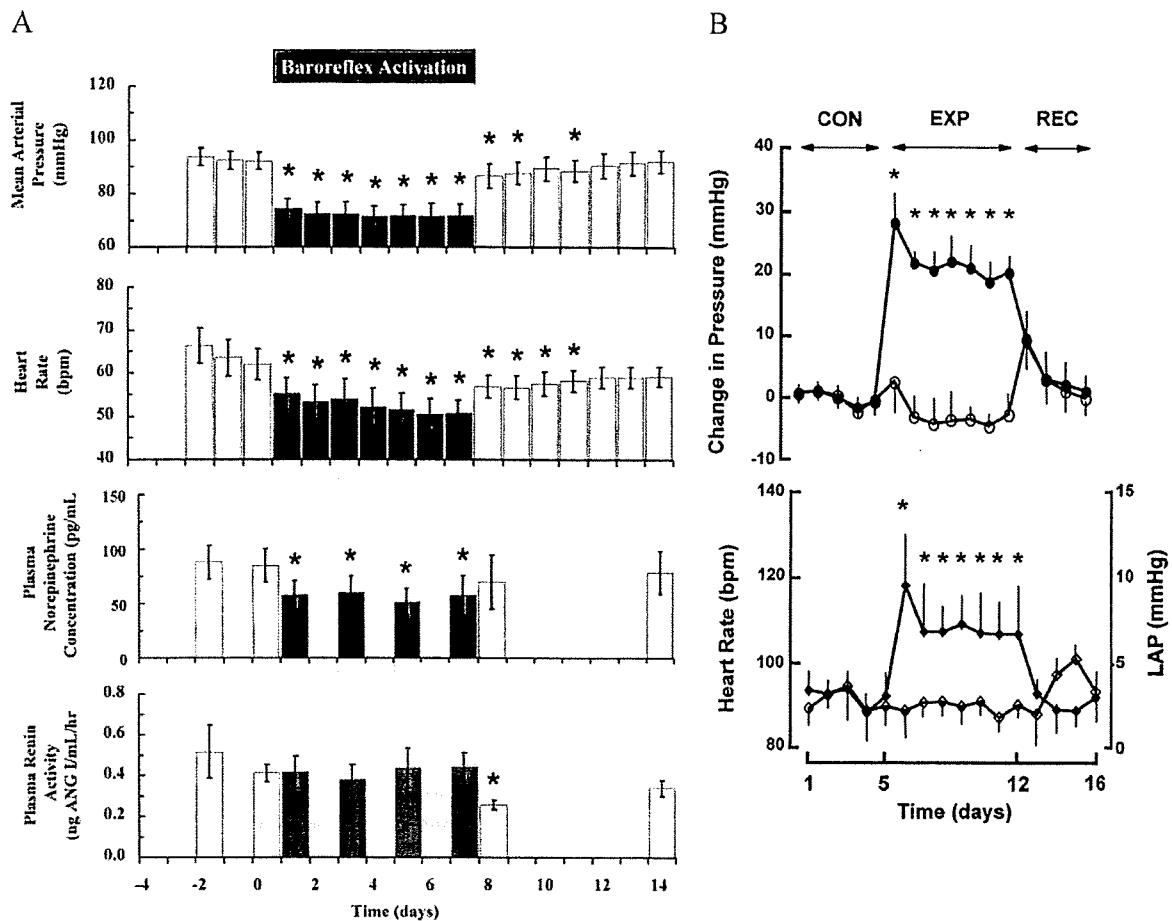


Fig. 4. (A) Effect of continuous baroreflex activation (bilateral carotid sinus stimulation) on mean arterial pressure, heart rate, plasma norepinephrine concentration, and plasma renin activity for seven days in six dogs. Due to decreased sympathetic activity, hypotension did not increase renin or decrease sodium excretion. (*) $p < 0.05$. (B) Chronic baroreceptor unloading (barodenervation and ligation of common carotid artery of the one remaining innervated carotid sinus) continuously increased blood pressure (closed circle) and heart rate (closed diamond) for seven days in dogs ($n = 5 \sim 6$). Open circle: carotid sinus pressure; open diamond: left atrial pressure (LAP). CON: control; EXP: baroreceptor unloading; REC: recovery; (*) $p < 0.05$. (Reproduced from [52] (A) and [58] (B) with permission.)

C. Electroacupuncture

Electrical acupuncture stimulation may be used to decrease blood pressure and decrease sympathetic nerve activity [67]–[70] [Fig. 5(A)]. Acupuncture stimulation changes the static properties of the central baroreflex controller in a direction of decreasing maximal sympathetic activity [67] [Fig. 5(A)] without changing the dynamic properties [68]. Kawada *et al.* [69] succeeded in developing a feedback depressor system by acupuncture in cats [Fig. 5(B)].

V. TREATMENT OF HYPOTENSION

Unlike hypertension, control of pressure against hypotension has been outside the scope of bionic cardiology. However, transient hypotension during, for example, postural change is one of the best targets for bionic cardiology for the following reasons. Severe orthostatic hypotension occurs as a result of damage to any of the components of the arterial baroreflex, including baroreceptors (neck surgery, radiation), vasomotor centers (Shy-Drager syndrome), and efferent pathways (spinal-cord injury). Hypotension is usually profound and requires prompt restoration with much shorter delay than is possible with any

available drug to avoid syncope. Chronic pressor treatments should be avoided, as continuous hypertension increases the risk for atherosclerosis. For the above reasons, pharmacological treatments, either continued or on-demand, are obviously inappropriate. As patients may lose consciousness with sudden hypotension, fully automatic feedback control of pressure should be developed.

A. Open-Loop Characterization of Baroreflex System

To accomplish feedback pressure control, Sato *et al.* [10] and Kawada *et al.* [11] analyzed static open-loop characteristics of the two subsystems of the baroreflex: controller (discharging sympathetic nerve traffic in response to sensed pressure) and plant (changing pressure according to sympathetic nerve traffic). The actual operating pressure is determined by the intersection (i.e., equilibrium) between the two functional curves of subsystems. Sato *et al.* [12] and Ikeda *et al.* [13] analyzed the open-loop transfer functions over a wide frequency range. They demonstrated that the transfer function of the plant approximates a second order low-pass filter. In contrast, they demonstrated that the transfer function of the controller possesses derivative characteristic. By analyzing

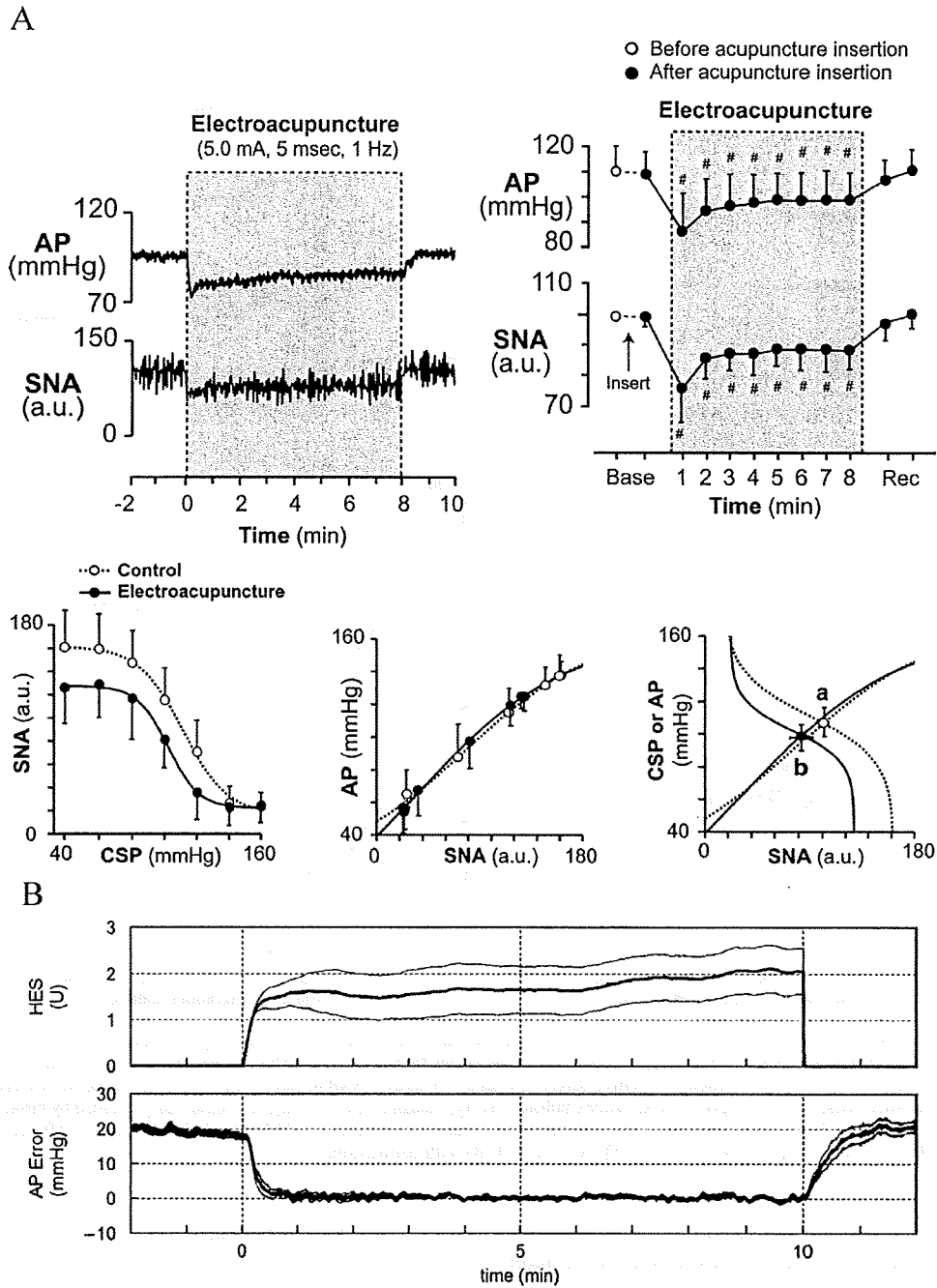


Fig. 5. (A) Electroacupuncture at Zusanli acupoint decreases arterial pressure (AP) and cardiac sympathetic nerve activity (SNA) for 8 min in six rabbits with intact baroreflex (top). Left: a representative example; right: pooled data (#) $p < 0.05$ versus baseline after acupuncture insertion. Hypotensive and sympathoinhibitory effect were due to the changes in controller (bottom left) but not plant (bottom center) of baroreflex. CSP: carotid sinus pressure. (B) Feedback control of AP by acupuncture-like hind-limb electrical stimulation (HES) in eight cats. Changes in HES is translated into changes in stimulus intensity (if $HES > 1$) and into changes in stimulus frequency (if $HES < 1$). (Reproduced from [67] (A) and [69] (B) with permission.)

these transfer functions, Ikeda *et al.* [13] have shown that the normal biological baroreflex is optimal to achieve quick and stable closed-loop responses.

B. Bionic Feedback Pressure Regulation

With the basic data at hand [14], Sato *et al.* [5], [6] designed a bionic baroreflex system by mimicking the functional biological baroreflex. The controller was designed so that the transfer function of the cascade of the controller and the biological plant

(for stimulation of sympathetic celiac ganglion) matches that of the total-loop baroreflex. Therefore, the transfer function of the desired controller was obtained from the ratio of the transfer function of total-loop baroreflex to that of the plant. In ten rats depleted of functional baroreflex [6], the application of bionic baroreflex during a head-up tilt significantly ($p < 0.05$) attenuated blood pressure drop from 34 ± 6 to 21 ± 5 mmHg at 2 s, and from 52 ± 5 to 15 ± 6 mmHg at 10 s. The residual pressure drop was not different from that observed in rats with intact baroreflex [Fig. 6(A)].

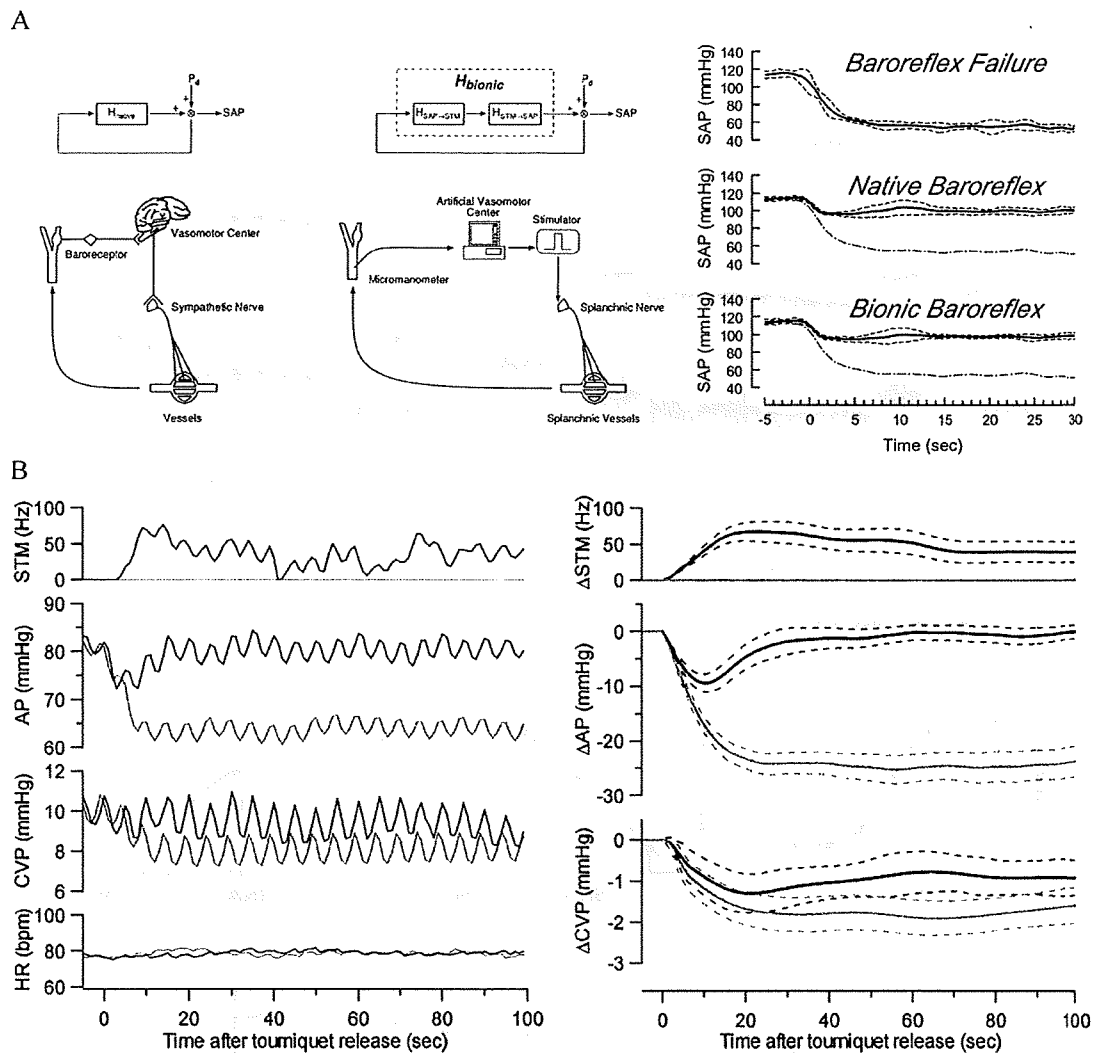


Fig. 6. (A) Functional and anatomical diagram of native baroreflex (left) and bionic baroreflex (center). Pd: pressure perturbation; SAP: systemic arterial pressure; H_{native} : open-loop transfer function of native baroreflex; H_{bionic} : open-loop transfer function of total bionic baroreflex; $H_{\text{SAP} \rightarrow \text{STM}}$: transfer function of designed bionic baroreflex controller; $H_{\text{STM} \rightarrow \text{SAP}}$: transfer function of native baroreflex plant. Changes in SAP in baroreflex failure, native baroreflex, and bionic baroreflex after head-up tilt (right). Dash-dot lines: average response in baroreflex failure. (B) Hypotension after tourniquet release was prevented by bionic baroreflex system using epidural spinal cord stimulation. Left: a representative patient; right: pooled data from 21 patients. STM: stimulation frequency; AP: arterial pressure; CVP: central venous pressure, HR: heart rate. (Reproduced from [5], [6] (A) and [72] (B) with permission.)

Yanagiya *et al.* [71] constructed a bionic baroreflex system using spinal cord stimulation via an epidural electrode catheter in six cats. They [71] designed the controller to provide quick and stable control only, rather than to mimic the biological controller. The system ameliorated a drop in pressure from 37 ± 5 to 21 ± 2 mmHg at 5 s and 59 ± 11 to 8 ± 4 mmHg at 30 s ($p < 0.05$). Epidural spinal-cord stimulation was further clinically applied by Yamasaki *et al.* [72] during surgery in a selected group of patients ($n = 12$) undergoing knee surgery. Pressure drop after tourniquet deflation was suppressed significantly ($p < 0.05$) from 17 ± 3 to 9 ± 2 mmHg at 10 s and 25 ± 2 to 1 ± 2 mmHg at 50 s [Fig. 6(B)]. Various inputs other than direct sympathetic stimulation may change blood pressure [67]–[70], [73]–[75]. Even noninvasive transcutaneous electrical stimulation [76] was developed for suppressing hypotension in patients with spinal-cord injury. In 12 patients, bionic feedback control restored the pressure drop by 50% in 35 ± 12 s and by 90% in 60 ± 18 s.

VI. TREATMENT OF HEART FAILURE

A. Neurohormonal Activation Plays Major Roles in the Pathogenesis of Heart Failure

Heart failure is a complex syndrome that can result from any kind of cardiac diseases at their advanced stage. Mortality with this syndrome is considerably high even with the development of state-of-art treatments including artificial hearts, regenerative medicine, and cardiac transplantation. Recently, implantable device-based treatment of heart failure has attracted physicians' interest because of its enormous impact on survival. Available devices include implantable cardiac defibrillator to terminate fatal arrhythmia and cardiac resynchronization treatment device to improve the synchronicity of left ventricular contraction and hence cardiac performance. Device for bionic treatment of heart failure is now under aggressive development to complement the roles of these devices.